



# TGF- $\beta$ *sensu stricto* signaling regulates skeletal morphogenesis in the sea urchin embryo



Zhongling Sun, Charles A. Etensohn\*

Department of Biological Sciences, Carnegie Mellon University, 4400 Fifth Avenue, Pittsburgh, PA 15213, United States

## ARTICLE INFO

### Keywords:

Sea urchin embryo  
Primary mesenchyme cells  
Skeleton  
Morphogenesis  
Biomineralization  
TGF- $\beta$  signaling

## ABSTRACT

Cell-cell signaling plays a prominent role in the formation of the embryonic skeleton of sea urchins, but the mechanisms are poorly understood. In the present study, we uncover an essential role for TGF- $\beta$  *sensu stricto* signaling in this process. We show that TgfbtII, a type II receptor dedicated to signaling through TGF- $\beta$  *sensu stricto*, is expressed selectively in skeletogenic primary mesenchyme cells (PMCs) during skeleton formation. Morpholino (MO) knockdowns and studies with a specific TgfbtII inhibitor (ITD-1) in both *S. purpuratus* and *Lytechinus variegatus* embryos show that this receptor is required for biomineral deposition. We provide pharmacological evidence that Alk4/5/7 is the cognate TGF- $\beta$  type I receptor that pairs with TgfbtII and show by inhibitor treatments of isolated micromeres cultured *in vitro* that both Alk4/5/7 and TgfbtII function cell-autonomously in PMCs. Gene expression and gene knockdown studies suggest that TGF- $\beta$  *sensu stricto* may be the ligand that interacts with TgfbtII and support the view that this TGF- $\beta$  superfamily ligand provides an essential, permissive cue for skeletogenesis, although it is unlikely to provide spatial patterning information. Taken together, our findings reveal that this model morphogenetic process involves an even more diverse suite of cell signaling pathways than previously appreciated and show that PMCs integrate a complex set of both generalized and spatially localized cues in assembling the endoskeleton.

## 1. Introduction

The formation of the skeleton is a prominent morphogenetic event during sea urchin embryogenesis (Wilt and Etensohn, 2007; Etensohn, 2013; McIntyre et al., 2014; McClay, 2016). The skeleton is produced exclusively by the primary mesenchyme cell (PMC) lineage, which arises from the micromeres of the 16-cell stage embryo. During gastrulation, PMCs ingress into the blastocoel and adopt a stereotypical, ring-like arrangement along the blastocoel wall. This cellular pattern, known as the subequatorial PMC ring, is composed of two ventrolateral cell clusters (VLCs) linked by dorsal and ventral cell chains. As the subequatorial ring forms, filopodia extended by the PMCs fuse, creating a cable-like structure (the pseudopodial cable) that joins the cells in a syncytial network (Hodor and Etensohn, 2008; Etensohn and Dey, 2016). Skeletogenesis begins with the formation of one tri-radiate spicule rudiment within each VLC. The three arms of each rudiment subsequently elongate and branch in a characteristic pattern, producing the two mirror-image spicules of the pre-feeding pluteus larva. Each spicule is a network of interconnected, linear skeletal rods; these include the body rods, which extend into the dorsal apex, and the postoral and anterolateral rods, which support the arms that extend from the ventral

surface of the larva. For the most part, the deposition of skeletal rods occurs within the pre-formed PMC pseudopodial cable, the location of which therefore determines the spatial arrangement of the rods. The rods in the larval arms, however, extend outward through the addition of biomineral by a “plug” of PMCs located at the growing tips. The skeleton gives the early larva its easel-like shape and influences its orientation, swimming and feeding (Hart and Strathmann, 1994; Pennington and Strathmann, 1990; Strathmann, 1971; Strathman and Grunbaum, 2006; Adams et al., 2011).

PMCs maintain close contact with the overlying ectodermal epithelium throughout development. It is perhaps not surprising, then, that skeletal growth and patterning are tightly regulated by cues from the ectoderm. Early studies documented a localized thickening of the ectoderm overlying the VLCs (Gustafson and Wolpert, 1961; Galileo and Morrill, 1985) and the formation of supernumerary tri-radiate spicules in embryos with ventralized ectoderm (Hardin et al., 1992; Armstrong et al., 1993). Furthermore, photoablation of a patch of ectodermal cells at the tip of the postoral arms prevents the elongation of the underlying rod, suggesting that short-range, ectoderm-derived cues are required for skeletal elongation (Etensohn and Malinda, 1993). Stereotypical variations in the elongation rates of the various

\* Corresponding author.

E-mail address: [ettensohn@cmu.edu](mailto:ettensohn@cmu.edu) (C.A. Etensohn).

<http://dx.doi.org/10.1016/j.ydbio.2016.12.007>

Received 22 August 2016; Received in revised form 5 December 2016; Accepted 5 December 2016

Available online 10 December 2016

0012-1606/ © 2016 Elsevier Inc. All rights reserved.

skeletal rods observed *in vivo* also provide evidence that local cues regulate skeletal growth (Guss and Ettensohn, 1997). More recent studies have shown that VEGF3, which is expressed by sub-territories of the ectoderm overlying sites of skeletal growth and branching, is a critically important cue with multiple effects on PMC migration and biomineral formation (Duloquin et al., 2007; Knapp et al., 2012; Adomako-Ankomah and Ettensohn, 2013; Sun and Ettensohn, 2014). Evidence suggests that other local ectodermal cues may play a role, including FGF, BMP5, and an unidentified signal emanating from the ectoderm of the dorsal apex, although these are less well defined (Röttinger et al., 2008; Adomako-Ankomah and Ettensohn, 2013; Sun and Ettensohn, 2014; Piacentino et al., 2016a). Recent studies have also pointed to the involvement of TGF- $\beta$  superfamily signaling in skeletogenesis. In *S. purpuratus*, the activity of Alk4/5/7 (a type I TGF- $\beta$  receptor) is required for skeletogenesis from the mesenchyme blastula stage (Bergeron et al., 2011), and in *L. variegatus*, late Alk4/5/7 activity is required for anterior skeletal patterning (Piacentino et al., 2015).

TGF- $\beta$  signaling is a multifunctional pathway that controls cell proliferation, cell differentiation and tissue homeostasis (Wu and Hill, 2009; Massagué, 2012; Hata and Chen, 2016). TGF- $\beta$  pathway genes are ubiquitous in the animal kingdom from basal metazoan species (*Trichoplax adhaerens*) to mammals (Huminiński et al., 2009). Phylogenetic analysis of the sea urchin (*Strongylocentrotus purpuratus*) genome has identified 14 genes encoding TGF- $\beta$  superfamily ligands (Lapraz et al., 2006). Nodal, Activin and TGF- $\beta$  *sensu stricto* (hereafter referred to as “TGF- $\beta$ ”) are among those ligands that signal through Alk4/5/7 and its downstream effector, Smad2/3. Nodal is the best-characterized TGF- $\beta$  superfamily ligand in the sea urchin and this signaling protein plays an essential role in establishing the dorsal-ventral and left-right axes (Duboc et al., 2004, 2005; Luo and Su, 2012). Activin plays a role in micromere-mediated endomesoderm specification (Sethi et al., 2009) and univin has been implicated in both dorso-ventral axis specification and skeletal development (Zito et al., 2003; Range et al., 2007; Piacentino et al., 2015). Sp-TGF- $\beta$  is the only member of this ligand subfamily in *S. purpuratus* and the first TGF- $\beta$  subfamily member identified in a non-chordate deuterostome (Lapraz et al., 2006). Sp-TGF- $\beta$  is expressed during embryogenesis (Tu et al., 2012, 2014) but its function has not been examined.

Type II receptors provide specificity for particular TGF- $\beta$  superfamily ligands. Three type II TGF- $\beta$  receptors have been identified in the *S. purpuratus* genome; Sp-Acvr2, Sp-Bmpr2, and Sp-TfgbrII (Lapraz et al., 2006). Based on ligand-receptor interactions in mammals (Yadin et al., 2016), it is likely that in sea urchins Nodal and Activin interact with the same type II receptor, Acvr2. This is consistent with the observation that overexpression of Activin has the same radializing effect on sea urchin embryos as overexpression of Nodal (Flowers et al., 2004; Duboc et al., 2010). In mammals, TGF- $\beta$  interacts specifically with a devoted type II receptor, TgfbriII, which recruits Alk4/5/7 and induces the phosphorylation of Smad2/3 (Boesen et al., 2002; Yadin et al., 2016).

In this study, we sought to explore further the cell signal-dependent regulation of skeletal morphogenesis in sea urchins. Our findings reveal an unexpected role for TGF- $\beta$  *sensu stricto* signaling in skeleton formation. We identify the receptors and the ligand that mediate this interaction and provide important information concerning the time and location of TGF- $\beta$  signaling during development. These findings add to our understanding of the complex role of extracellular signaling in regulating a model morphogenetic process.

## 2. Materials and methods

### 2.1. Embryo culture

Adult *Strongylocentrotus purpuratus* and *Lytechinus variegatus* were obtained and embryo cultures were established as described

previously (Adomako-Ankomah and Ettensohn, 2013). Embryos were cultured in artificial seawater (ASW) at 15 °C (*S. purpuratus*) or 19–23 °C (*L. variegatus*).

### 2.2. Cloning and probe synthesis

The complete coding sequence of *Sp-tgfbriII* was obtained by RT-PCR using *Sp-tgfbriII* forward primer-1 and reverse primer-1 (Supplementary Table 1), and cloned into the pCS2+ vector using the Xho I and NotI restriction sites. The construct was linearized with Xho I and digoxigenin (DIG)-labeled RNA probe was synthesized using the T3 MegaScript Kit (Ambion). The complete coding sequence of *Sp-TGF- $\beta$*  was obtained by RT-PCR with the *Sp-TGF- $\beta$*  forward and reverse primers (Supplementary Table 1) and cloned into pCS2+ vector using the Xba I and Eco RI restriction sites. The construct was linearized with Xba I and DIG-labeled probe was synthesized using the SP6 MegaScript Kit (Ambion).

### 2.3. Whole mount in situ hybridization (WMISH) and immunostaining

WMISH and fluorescence-based WMISH (F-WMISH) were performed as described previously (Sun and Ettensohn, 2014). *Lv-vegfb3* and *Lv-vegfr-10-Ig* WMISH probes were synthesized by Adomako-Ankomah (Adomako-Ankomah and Ettensohn, 2013). Immunostaining with monoclonal antibody 6a9 was carried out as described by Adomako-Ankomah and Ettensohn (2013).

### 2.4. Inhibitor studies

10 mM stock solutions of ITD-1 (Tocris Bioscience), SB431542 (Tocris Bioscience), SB525334 (Selleckchem) and RepSox (Selleckchem), and a 100 mM stock solution of Nifedipine (Tocris Bioscience) were prepared in DMSO and stored at –20 °C. Working solutions were prepared in ASW immediately before use. As controls, embryos were cultured in equivalent concentrations of DMSO.

### 2.5. Microinjection and microsurgery

Microinjection of morpholinos (MOs) (Gene Tools, LLC) into fertilized eggs was performed as previously described (Cheers and Ettensohn, 2004) except that *S. purpuratus* eggs were fertilized in the presence of 0.1% (wt/vol) para-aminobenzoic acid (PABA) to prevent hardening of the fertilization envelope. MO sequences and injection concentrations are provided in Supplementary Table 2. Microsurgical removal of PMCs from mesenchyme blastula stage embryos was carried out as described by Ettensohn and McClay (1988).

### 2.6. RT-PCR

RT-PCR analysis was performed as described previously (Adomako-Ankomah and Ettensohn, 2011). RNA was extracted from 150 control and 150 *Sp-tgfbriII* splice-blocking MO-injected *S. purpuratus* embryos using the Nucleospin RNA Plus kit (Clontech). cDNA was synthesized using the RETROscript Reverse Transcription Kit (Ambion), and PCR was performed using *Sp-tgfbriII* forward primer-2, reverse primer-2, and Platinum *Taq* High Fidelity DNA Polymerase (Invitrogen). PCR products were analyzed on 1% agarose gels that contained 0.5% ethidium bromide.

### 2.7. Micromere isolation and culture

Micromere isolation was carried out essentially as described by Wilt and Benson (2004). Dejellied *S. purpuratus* eggs (1 ml) were fertilized in ASW containing 0.1% (wt/vol) PABA. After fertilization, the PABA-containing ASW was replaced with calcium-free seawater (CFSW) and

the embryos were cultured with stirring. At the 8-cell stage, fertilization envelopes were removed by passing the embryos through 52  $\mu\text{m}$  nylon mesh. At the 16-cell stage, embryos were dissociated by repeated centrifugation and resuspension in CFSW and calcium/magnesium-free seawater (CMFSW). The final dissociation was carried out in 10 ml CFSW and the cell suspension was gently layered on a linear sucrose gradient (5–25% sucrose in CFSW) at 1g at 15 °C. 1% 1 M  $\text{CaCl}_2$  was added to isolated micromeres to restore cell adhesion. Micromeres were allowed to attach to the culture dish for 1 h and the fluid was aspirated and replaced by filtered ASW containing 100  $\mu\text{g}/\text{ml}$  streptomycin. At 24 h post-fertilization (hpf), cultured micromeres were supplemented with 4% (v/v) horse serum to allow spicule differentiation.

### 3. Results

#### 3.1. The expression of *Sp-tgfbprtII* is restricted to the skeletogenic PMC lineage

Transcriptome profiling of PMCs isolated at the mesenchyme blastula stage indicated that *Sp-tgfbprtII* mRNA was enriched in these cells (Rafiq et al., 2014). Based on the temporal expression data of Tu et al. (2012, 2014), *Sp-tgfbprtII* transcripts begin to accumulate at the blastula stage, peak at ~800 transcripts/embryo at the mesenchyme blastula stage (24 hpf), and then gradually decline to lower levels at post-gastrula stages. To study the spatial expression pattern of this gene in detail, we cloned the full-length (1788 bp) *Sp-tgfbprtII* coding sequence into pCS2+ and synthesized a digoxigenin-labeled RNA probe for WMISH analysis. WMISH analysis showed that *Sp-tgfbprtII* was first expressed selectively in PMC precursors at the hatched blastula stage (Fig. 1A). The expression level peaked at the mesenchyme blastula stage, when *Sp-tgfbprtII* mRNA appeared to be present in most or all PMCs (Fig. 1B). At the early gastrula stage, when the PMCs were beginning to form the subequatorial ring, PMCs on one side of the embryo (presumably the ventral side, based on the later pattern of expression) expressed higher levels of *Sp-tgfbprtII* mRNA than cells in the remainder of the ring (Fig. 1C). At the mid-gastrula stage, expression was highest in the VLCs, where skeletogenesis is initiated (Fig. 1D, D'). The expression of *Sp-tgfbprtII* at later stages was not detectable by WMISH (data not shown). The tightly regulated spatial and temporal expression of *Sp-tgfbprtII* suggested that this signaling receptor might play a role in skeletogenesis.

Structural analysis of the ligand binding domains of mammalian type II receptors has identified two disulfide bridges (C31–C48, C38–C44) that are unique to *TgfbprtII* (Boesen et al., 2002). To understand the divergence of *TgfbprtII* and *Acvr2* and possible ligand-type II receptor binding specificities in sea urchins, we aligned the amino acid sequences of *TgfbprtII* and *Acvr2* from two sea urchin species (*S. purpuratus* and *L. variegatus*) with the sequences of their human orthologs (Supplementary Fig. 1). The full-length coding sequences of *Lv-tgfbprtII* and *Lv-acvr2* were obtained by 5' RACE. We found that the positions of cysteine residues (and likely disulfide bridges) in *Sp-TgfbprtII* (C32–C59 and C39–C55) and *Lv-TgfbprtII* (C30–C57 and C37–C53) matched very closely those of human *TgfbprtII*, but these residues were absent from sea urchin *Acvr2*. This protein sequence alignment therefore provides evidence that *TgfbprtII* and *Acvr2* in the sea urchin are structurally distinct and suggests that they recognize different TGF- $\beta$  ligands. Our analysis supports the molecular phylogeny of Lapraz et al. (2006), which identified *Sp-TgfbprtII* as the ortholog of human TGF- $\beta$  receptor type II.

#### 3.2. *TgfbprtII* is required for skeletogenesis in *S. purpuratus* and *L. variegatus*

To study the function of *TgfbprtII* in the sea urchin embryo, we knocked down the expression of this protein in *S. purpuratus* using a splice-blocking MO (SB-MO) designed to overlap the exon 2-intron 2 boundary (Fig. 2E). We anticipated that this would lead to the exclusion of exon 2 (275 bp in length), thereby altering the reading frame and introducing multiple, in-frame stop codons. The predicted protein product is a short (15 amino acid), N-terminal fragment of the receptor that lacks the entire kinase domain. The effectiveness of the MO was assessed by RT-PCR analysis of 150 control embryos or 150 embryos injected with 2, 3, or 4 mM *Sp-tgfbprtII* MO. The observed shift in the size of the major PCR product (Fig. 2E, F) was consistent with the deletion of exon 2, which was confirmed by cloning and sequencing the PCR product. Small amounts of an uncharacterized, mis-spliced product slightly smaller than the wild-type mRNA were also detected which may indicate the utilization of a cryptic donor splice site within exon 2. The effect of the MO on splicing was dose dependent; at higher MO concentrations the mis-spliced form was predominant, although the knockdown was incomplete at all concentrations tested.

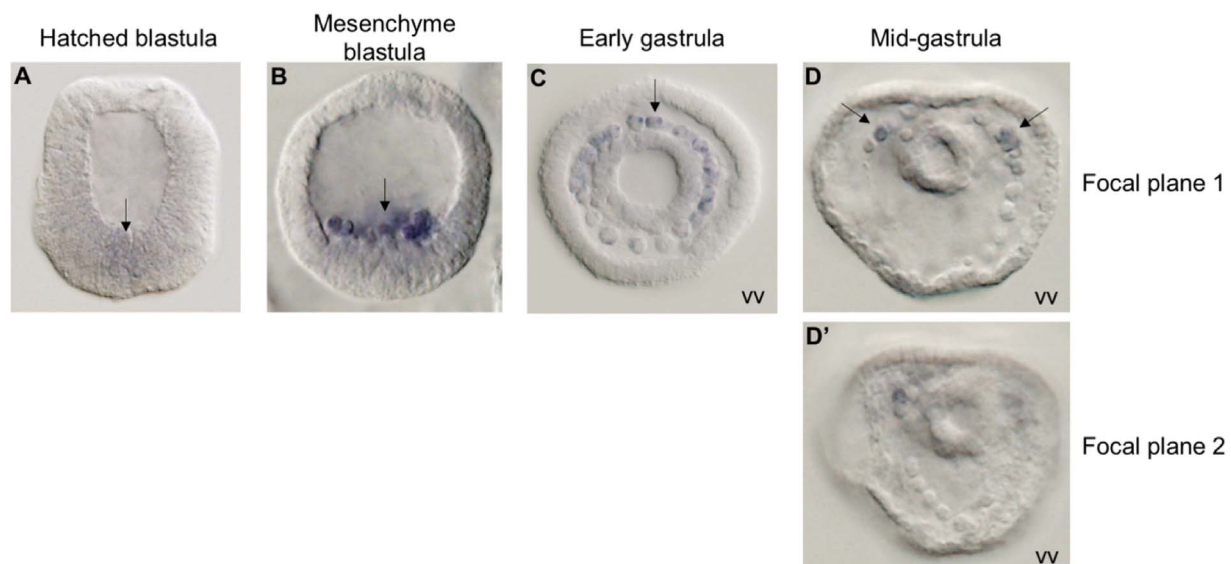


**Fig. 1.** *Sp-tgfbprtII* mRNA is enriched in PMCs. WMISH analysis shows that *Sp-tgfbprtII* mRNA is selectively expressed in PMC precursors at the hatched blastula stage (A), in most or all the PMCs at the mesenchyme blastula stage (B), in ventral PMCs at the early gastrula stage (C) and in the PMCs in the VLCs at the mid-gastrula stage (D, D'). vv=vegetal view. Arrows indicate cells expressing *Sp-tgfbprtII*.

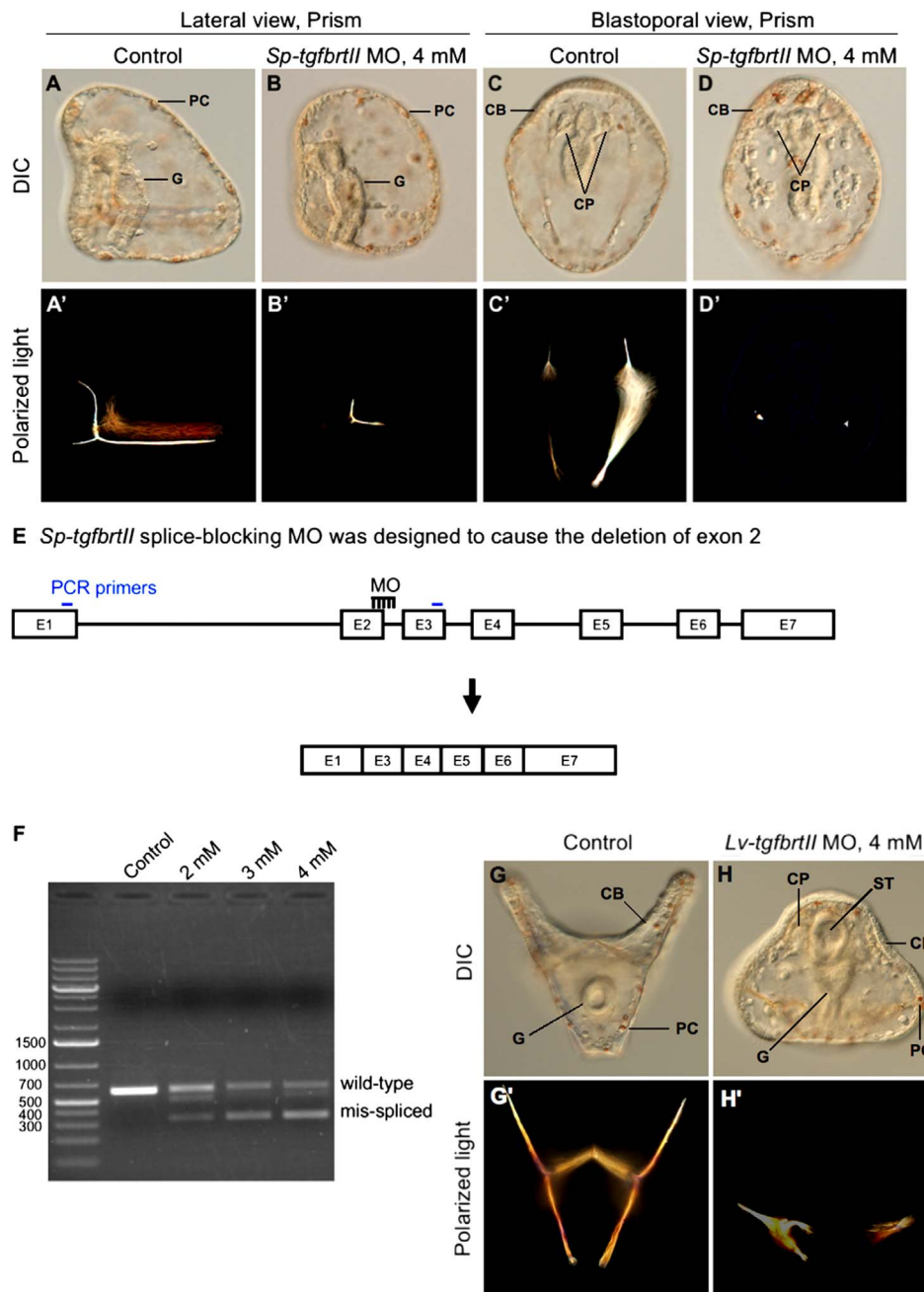


**Fig. 2.** Knockdown of *tgfbtIII* inhibits skeletogenesis in *S. purpuratus* (A–F) and *L. variegatus* (G–H') embryos. (A–D') DIC (A–D) and polarized light (A'–D') images of control *S. purpuratus* embryos and embryos injected with 4 mM *Sp-tgfbtIII* splice-blocking MO, viewed laterally and from the blastopore at the prism stage (60 hpf). Control embryos have extensive, branched skeletons, as revealed by polarized light (A', C'). In contrast, morphant embryos have only small birefringent granules or tri-radiate spicule primordia (B', D'), although these embryos exhibit other late embryonic structures. (E) Design of the *Sp-tgfbtIII* splice-blocking MO. (F) Agarose gel showing a dose-dependent deletion of exon 2 in morphant embryos. (G–H') DIC (G, H) and polarized light (G', H') images of a control *L. variegatus* embryo at the pluteus stage (blastoporal view) and a sibling embryo injected with 4 mM *Lv-tgfbtIII* translation-blocking MO (ventral view). The morphant embryo has a highly reduced skeleton but other post-gastrula structures are well-formed. CB = ciliary band, CP = coelomic pouch, G = tripartite gut, PC = pigment cell, ST = stomodeum.

Injection of 4 mM *Sp-tgfbtIII* SB-MO resulted in a significant inhibition of skeletal growth without affecting the specification, ingression or migration of PMCs. Light microscopic observations of living, morphant embryos showed that PMCs ingressed in normal numbers and adopted a typical ring-like configuration during gastrulation. Skeletal development was impaired in such embryos, however, and most formed small spicule triradiates or tiny skeletal granules (90% of embryos scored, n=97) (Fig. 2B, B' D, D'). Injection with the SB-MO at lower concentrations (2 mM and 3 mM) also inhibited skeletal growth but to a lesser extent, resulting in truncated skeletons. The development of other tissues including pigment cells, the gut, coelomic

pouches and ciliary band appeared normal in morphant embryos.

We also designed a translation-blocking MO (TB-MO) to knock down *tgfbtIII* expression in a different sea urchin species, *L. variegatus*. Skeletogenesis in embryos injected with 4 mM *Lv-tgfbtIII* was severely inhibited (Fig. 2G–H'); at the prism stage, when control embryos had developed large, branched skeletons, 88% of morphant embryos had only small spicule triradiates or tiny skeletal granules (n=102). This experiment was informative in two ways. First, it revealed that the role of *TgfbtIII* in skeletal growth is conserved, at least in these two echinoid species. Second, it served as a control for the specificity of the *tgfbtIII* knockdown, as the sequences of the *S.*

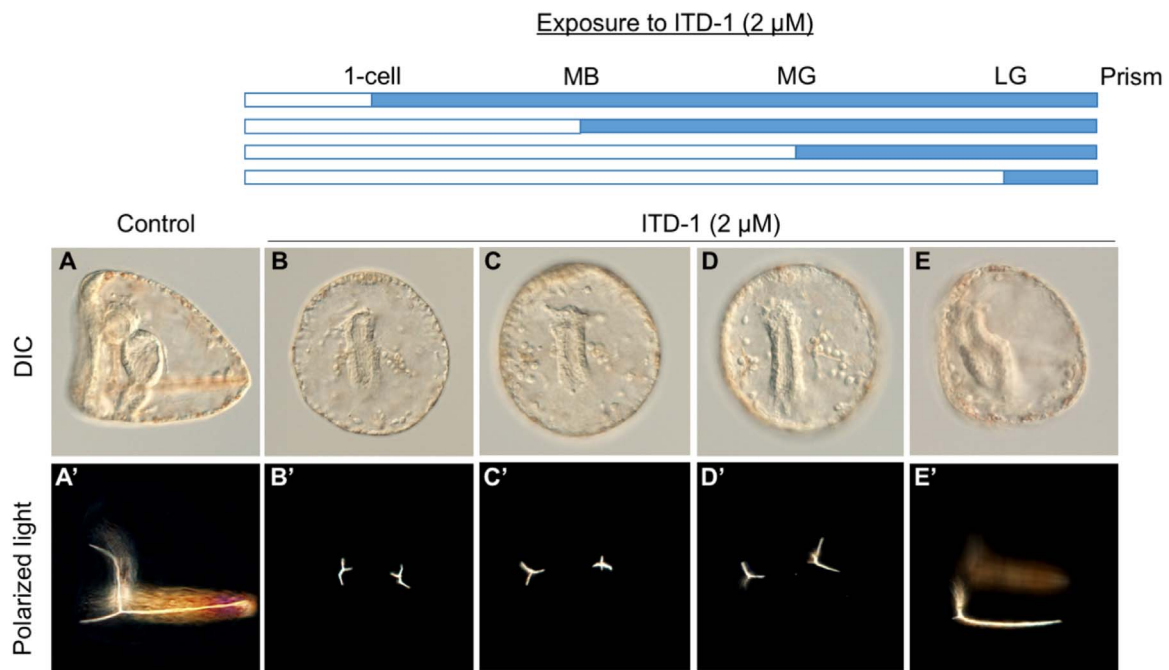


**Fig. 3.** Signaling via *TgfbrrtII* is required during gastrulation for skeletogenesis in *S. purpuratus*. DIC (A–E) and polarized light (A'–E') images of a control embryo (A, A') and embryos treated with 2  $\mu$ M ITD-1 at the 1-cell stage (B, B'), the mesenchyme blastula (MB) stage (24 hpf) (C, C'), the mid-gastrula (MG) stage (30 hpf) (D, D') or the late gastrula (LG) stage (40 hpf) (E, E'). All embryos were examined at the prism stage (50 hpf).

*purpuratus* and *L. variegatus* MOs were completely different, yet the two MOs had very similar, selective effects on skeletal growth.

### 3.3. Signaling through *TgfbrrtII* is required during gastrulation

As an alternative approach for testing the role of *TgfbrrtII* in skeletogenesis, and to examine the temporal requirements for signaling through the receptor, we used a newly developed, highly selective *TgfbrrtII* inhibitor, ITD-1. In mammalian cells, this drug enhances the proteasomal degradation of *TgfbrrtII*, clearing the protein from the cell surface and specifically blocking the phosphorylation of Smad2/3 via TGF- $\beta$  (but not Activin A) (Willems et al., 2012).

In preliminary studies, we examined the concentration-dependent effects of ITD-1 on the development of both *S. purpuratus* and *L. variegatus*. Embryos treated continuously from the mesenchyme blastula or early gastrula stage with sub-micromolar concentrations of ITD-1 (or with DMSO alone) gave rise to normal pluteus larvae. Embryos treated with 1  $\mu$ M ITD-1, however, showed a reproducible, partial inhibition of skeletal growth. Embryos treated with 2  $\mu$ M (*S. purpuratus*) or 5  $\mu$ M (*L. variegatus*) ITD-1 showed an almost complete inhibition of skeletal deposition, although small tri-radiate rudiments always formed. This concentration is close to the IC50 of the drug (~1  $\mu$ M) (Willems et al., 2012). Embryos exposed to these concentrations of ITD-1 swam normally, gastrulated on schedule, and developed a segmented gut, dorsal pigmentation, a complete ciliary band, two coleomic pouches, and a ventrally-positioned stomodeum (Supplemental Fig. 2A–E'). We immunostained embryos with monoclonal antibody 6a9, a marker for PMCs, and found that ITD-1 did not block PMC migration or prevent these cells from forming their characteristic subequatorial ring pattern (Supplemental Fig. 2F–G'). The one morphological difference we detected (other than the inhibition of skeletogenesis) was that the midgut (stomach) was not as expanded in ITD-1-treated embryos as in controls. These observations showed that ITD-1 selectively affected skeleton formation without affecting the development of many other tissues, arguing strongly that the effects on skeletogenesis were not due to general, toxic effects. These findings were also consistent with those of Willems et al. (2012) who showed no measurable toxic effects on mammalian cells at

concentrations as high as 10  $\mu$ M ITD-1, the highest concentration they assayed. We found that embryos treated with 10 or 20  $\mu$ M ITD-1 showed the same phenotype; *i.e.*, the deposition of two small spicule primordia that failed to elongate, without obvious effects on other tissues. We chose to use 2  $\mu$ M (*S. purpuratus*) or 5  $\mu$ M (*L. variegatus*) for most experiments, as these concentrations produced a robust inhibition of skeletogenesis in >90% of embryos from multiple batches.

Since ITD-1 is a chemical derivative of nifedipine, an L-type calcium channel blocker, and because calcium influx is likely to be required for the deposition of the calcium carbonate-based endoskeleton, we compared the effects of ITD-1 and nifedipine on skeletogenesis. A previous study showed that nifedipine effectively blocked skeletogenesis in *Hemicentrotus pulcherrimus* when used at concentrations of 100  $\mu$ M or higher (Dale et al., 1997). ITD-1 is about 50% less potent than nifedipine in blocking calcium transients of mammalian cardiomyocytes when used at 10  $\mu$ M, and both drugs have only very slight effects on calcium levels when used at 1  $\mu$ M (Willems et al., 2012). Mesenchyme blastula stage *S. purpuratus* embryos were treated with ITD-1 or nifedipine at concentrations of 1, 5 and 20  $\mu$ M. We found that 1  $\mu$ M ITD-1 had a pronounced, inhibitory effect on skeletogenesis while nifedipine had no effect at this concentration or at 5  $\mu$ M and only a very slight inhibition of skeletal elongation at 20  $\mu$ M (Supplemental Fig. 3). At higher concentrations, nifedipine blocked skeletogenesis almost completely, as originally reported by Dale et al. (1997). These results strongly suggest that ITD-1 inhibits skeletogenesis not by blocking calcium channels but by an alternative mechanism. Our findings are consistent with the observations of Willems et al. (2012), who demonstrated that ITD-1 acts by a mechanism independent of calcium transport.

In time-course studies, *S. purpuratus* embryos were treated with 2  $\mu$ M ITD-1 from the 1-cell (0.5 hpf), mesenchyme blastula (24 hpf), mid-gastrula (30 hpf), or late gastrula stage (40 hpf) until the prism stage (50 hpf), when the embryos were collected for analysis (Fig. 3). We found that treatment beginning at the mesenchyme blastula or early gastrula stages produced the same effect on skeletal growth as continuous treatment beginning at fertilization; *viz.*, only small skeletal triradiates were produced, similar to the effect of *Sp-tgfbrrtII* knock-down (over 90% of embryos, n > 100) (Fig. 3B, B' C, C'). This is

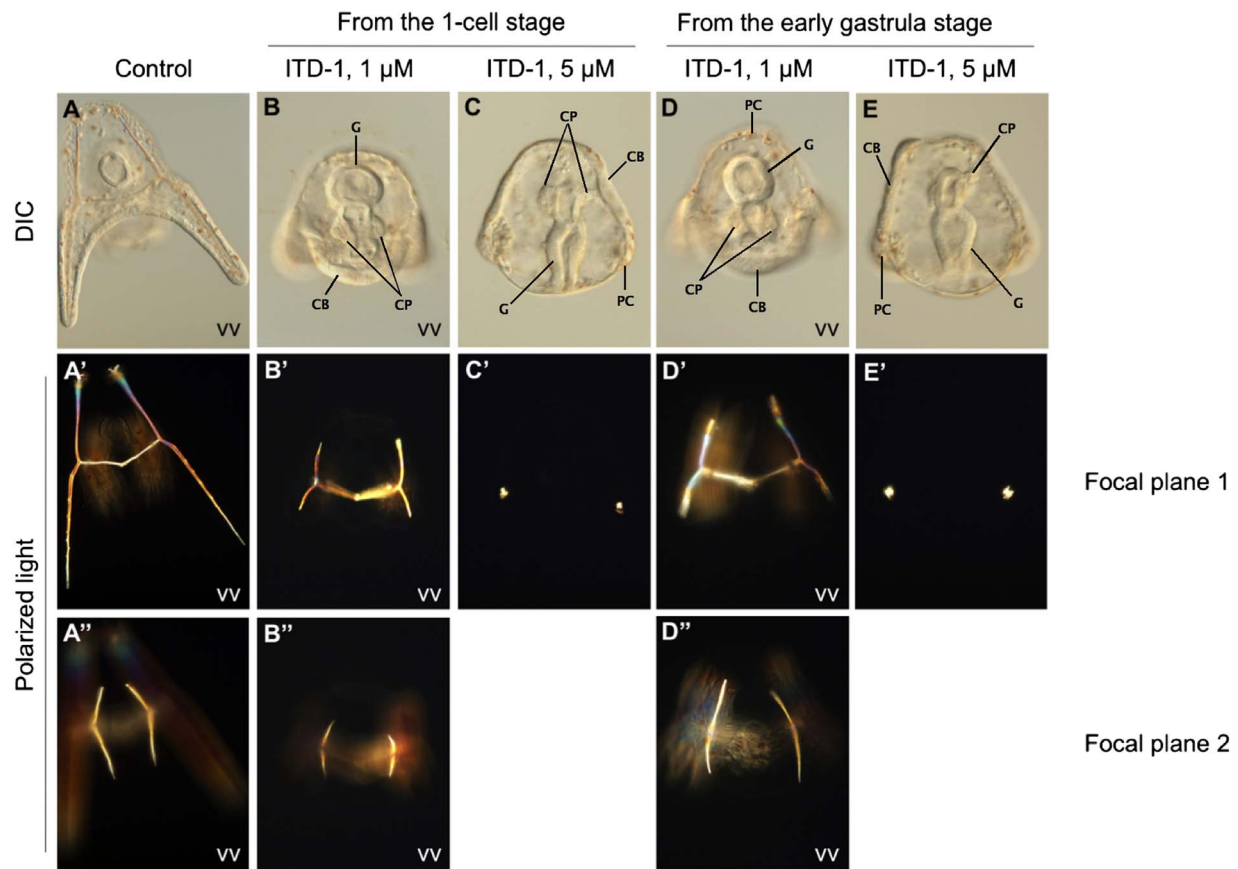


**Fig. 4.** *TgfbtII* is required for skeletogenesis in *L. variegatus*. DIC (top row) and polarized light (bottom rows) images of a control embryo (A–A'') and embryos treated with 1  $\mu$ M or 5  $\mu$ M ITD-1 from the 1-cell stage (B–C') or early gastrula (D–E') stages. All embryos were examined when controls had reached the pluteus stage (48 hpf). The lack of skeletal development in the ITD-1-treated embryos is not due to a general developmental delay, as shown by the formation of post-gastrula structures including the ciliary band (CB), coelomic pouches (CP), dorsal pigment cells (PC) and a compartmentalized gut (G).

consistent with the temporal expression of *Sp-tgfbtII*, which is not expressed until the blastula stage and peaks in expression early in gastrulation. When embryos were treated with 2  $\mu$ M ITD-1 at the mid-gastrula stage, after a birefringent granule was already present in each VLC, very limited skeletal growth occurred and only small triradiate skeletal rudiments were detected at 50 hpf (Fig. 3D, D'). In embryos treated at the late gastrula stage, however, after a small, triradiate spicule rudiment had already formed in each VLC, more significant elongation of all skeletal rods was detected, although each rod was significantly shorter than in control embryos (over 90% of embryos,  $n > 100$ ) (Fig. 3E, E'). Significantly, we also noted that exposure to ITD-1 from fertilization did not disrupt dorsal-ventral patterning in *S. purpuratus*, demonstrating that this drug does not inhibit the type II receptor activated by Nodal signaling (Duboc et al., 2004), which is presumably *Acvr2*.

Treatment of *L. variegatus* embryos with ITD-1 resulted in very similar effects (Fig. 4). We detected no difference in the development of embryos treated from the 1-cell stage or early gastrula stage and found that signaling is required during gastrulation in this species. As in *S. purpuratus*, early exposure to ITD-1 did not affect dorsal-ventral patterning in *L. variegatus*.

Previous studies have shown that microsurgical removal of PMCs at the mesenchyme blastula stage causes non-skeletogenic mesoderm (NSM) cells to alter their developmental program and adopt a skeletogenic fate (Ettensohn and McClay, 1988; Sharma and Ettensohn, 2011). We used *L. variegatus* embryos, which are highly amenable to microsurgical manipulation, to test whether signaling through *TgfbtII* was required for skeletogenesis by transfected NSM cells. PMCs were removed from mesenchyme blastula stage embryos and 6 h later (after NSM fate switching but before the onset of overt

skeletogenesis), half of the embryos were placed in 5  $\mu$ M ITD-1 while the others were allowed to continue development in normal seawater. 18 h after PMC removal, control PMC(-) embryos (9/9) had elaborate skeletons, while PMC(-) embryos (10/10) exposed to ITD-1 contained only tiny birefringent granules or very small spicules (Supplementary Fig. 4). Although they did not form a skeleton, ITD-1-treated PMC(-) embryos swam actively, gastrulated, and developed a tri-partite gut, ciliary band, and dorsal pigmentation.

#### 3.4. ITD-1 does not block skeletogenesis by altering *veg3/vegfr-10-Ig* expression

VEGF signaling plays a critically important role in PMC migration and skeletogenesis (Duloquin et al., 2007; Adomako-Ankomah and Ettensohn, 2013; Sun and Ettensohn, 2014). To test whether *TgfbtII* might be affecting skeletogenesis indirectly via effects on VEGF signaling, we examined the expression of *Lv-veg3* and *Lv-vegfr-10-Ig* in embryos exposed to ITD-1 from the 1-cell stage to the late gastrula stage. Two-color F-WMISH analysis indicated that both *Lv-veg3* and *Lv-vegfr-10-Ig* were expressed similarly in ITD-1-treated and control embryos (Fig. 5). As reported previously, *Lv-vegfr-10-Ig* was expressed preferentially by PMCs in the VLCs and *Lv-veg3* was expressed in the ectoderm overlying the PMC clusters. This result indicated that the inhibition of skeletogenesis by ITD-1 was not due to mis-regulation of *veg3/vegfr-10-Ig* expression.

#### 3.5. Late *Alk4/5/7* activity is required for skeletogenesis

*Alk4/5/7* is the TGF- $\beta$  type I receptor in sea urchins predicted to interact with the TGF- $\beta$  ligand-T $\beta$ R $\text{II}$  complex, based on known ligand-

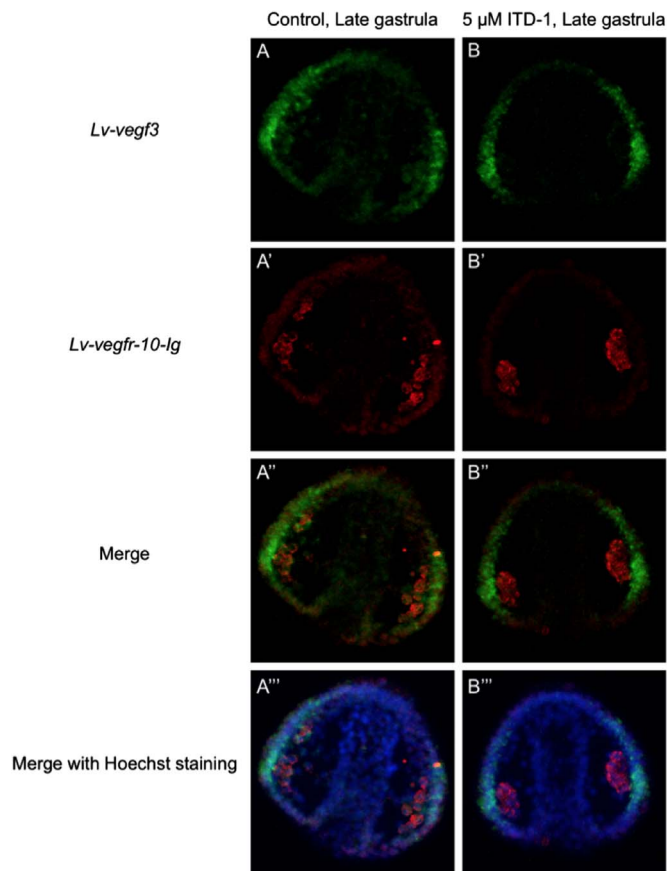


**Fig. 5.** The spatial expression patterns of *Lv-vegf3* and *Lv-vegfr-10-Ig* are not affected by ITD-1. Two-color, fluorescent WMISH analysis of *Lv-vegf3* (A, B) and *Lv-vegfr-10-Ig* (A', B') expression in a control late gastrula (A-A''') and a late gastrula that had been treated with 5 μM ITD-1 from the 1-cell stage (B-B''').

receptor interactions in mammals (Yadin et al., 2016). Alk4/5/7 probably also pairs with Acvr2, however, and is required during early development for Nodal signaling and dorsal-ventral axis formation (Range et al., 2007). A recent study concluded that late activity of Alk4/5/7 is also required for anterior skeletal patterning in *L. variegatus* (Piacentino et al., 2015). To investigate further the role of Alk4/5/7-mediated signaling in skeletogenesis, we used three highly specific and potent Alk4/5/7 inhibitors, SB431542, SB525334 and RepSox (Inman et al., 2002; Gellibert et al., 2004; Grygielko et al., 2005; Ogunjimi et al., 2012). *S. purpuratus* embryos were treated with Alk4/5/7 inhibitors at different concentrations beginning at the mesenchyme blastula stage to avoid effects on dorsal-ventral axis specification (Fig. 6A–G, A'–G'). We found that at low concentrations these inhibitors primarily affected the formation of the anterolateral rods without affecting the elongation of the body rod (Fig. 6B', D', F'), similar to the previously reported effects of 3 μM SB431542 in *L. variegatus* (Piacentino et al., 2015). We observed this selective effect, however, at a concentration of SB431542 that others have shown is too low to fully inhibit Alk4/5/7 activity, as assayed by dorsal-ventral polarity and SMAD phosphorylation (Ohguro et al., 2011; Bergeron et al., 2011). At slightly higher concentrations, *viz.*, concentrations that have been routinely used in other studies to inhibit Alk4/5/7 (*e.g.*, Duboc et al., 2005; Yaguchi et al., 2006; Bergeron et al., 2011; Luo and Su, 2012), all three inhibitors blocked the formation of all skeletal rods (over 90% of embryos,  $n > 200$ ) (Fig. 6C', E', G'). Surprisingly, in embryos exposed to RepSox, small birefringent granules were deposited within pigment cells, an effect that we have not examined further (Fig. 6G'). We also exposed *L. variegatus* embryos to Alk4/5/7 inhibitors during gastrulation and detected a pronounced inhibition of skeletogenesis (Fig. 6H–K, H'–K'). The formation of birefringent

granules in pigment cells was also detected in RepSox-treated *L. variegatus* embryos (Fig. 6K'). These findings provide strong evidence that signaling through Alk4/5/7 during gastrulation is required for skeletogenesis.

### 3.6. TGF- $\beta$ receptors function cell-autonomously in PMCs

As Alk4/5/7 is expressed in all three germ layers, including PMCs (Piacentino et al., 2015), we wondered whether Alk4/5/7 functions in PMCs to regulate skeletogenesis or acts indirectly through signaling processes in other cells. Furthermore, although WMISH analysis showed clearly that *tgfbprtII* is expressed selectively by PMCs, we could not formally exclude the possibility that low levels of the receptor were also present in other cells. To determine whether TGF signaling acts cell-autonomously in PMCs, we examined the effects of SB431542 (one of the Alk4/5/7 inhibitors) and ITD-1 on skeletogenesis by isolated micromeres cultured *in vitro*. We exposed micromeres isolated from 16-cell stage *S. purpuratus* embryos to 5 μM SB431542 or 5 μM ITD-1 from the equivalent of the mesenchyme blastula stage (18 h after plating) until the 4th day after fertilization. In these studies, we used a slightly higher concentration of ITD-1 than in previous experiments (5 μM instead of 2 μM) because we found that micromere culture medium, which contains horse serum, slightly attenuated the effects of ITD-1, perhaps because it contains exogenous TGF- $\beta$  ligands. In preliminary studies, we observed that 2 μM ITD-1 was less effective at preventing skeletal elongation in whole embryos when horse serum was present (Supplementary Fig. 5B, B', F, F'). For embryos cultured in micromere culture medium, 5 μM ITD-1 mimicked the effects observed when embryos in normal ASW were treated with 2 μM ITD-1 (Supplementary Fig. 5B, B', G, G'). Micromere culture medium did not, however, diminish the inhibitory effect of SB431542 on skeletogenesis in whole embryos (Supplementary Fig. 5D, D', H, H').

In multiple independent trials, we found that spicules produced by micromeres cultured in the presence of SB431542 or ITD-1 were significantly shorter than those produced by micromeres in culture medium alone ( $P < 0.0001$ ) (Fig. 7). These observations demonstrate a cell-autonomous function of Alk4/5/7 and *TgfbprtII* in skeletal elongation and show that these receptors mediate skeletal deposition by mechanisms independent of PMC positioning.

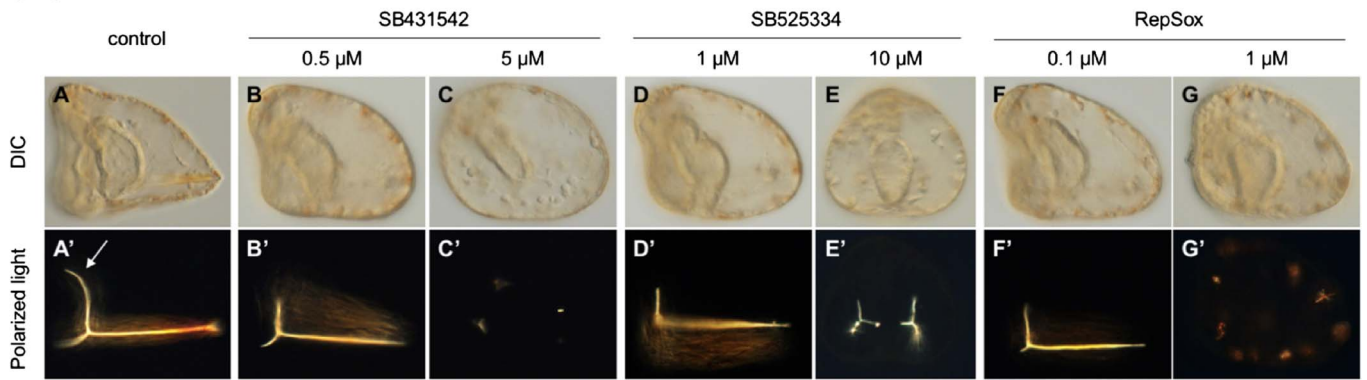
### 3.7. TGF- $\beta$ is required for skeletal elongation in the sea urchin embryo and is a candidate ligand for *TgfbprtII*

Analysis of TGF- $\beta$  signaling in mammals indicates that T $\beta$ RII interacts specifically with TGF- $\beta$  *sensu stricto* ligands and typically partners with T $\beta$ RI/Alk5 and Smads 2 and 3 to mediate signaling (Yadin et al., 2016). There is a single TGF- $\beta$  *sensu stricto* ligand in sea urchins, designated TGF- $\beta$  by Lapraz et al. (2006) and annotated as TGFb or TGFb2 by the sea urchin genome project (www.echinobase.org). There is no detectable maternal *tgf- $\beta$*  mRNA but expression increases during early development and peaks during gastrulation at ~250 transcripts/embryo (Tu et al., 2014).

WMISH analysis indicated that *tgf- $\beta$*  has a dynamic and complex pattern of expression during embryogenesis (Fig. 8). At the mesenchyme blastula stage, we detected faint WMISH signal predominantly in the PMCs but during early gastrulation signal was highest in the wall of the archenteron. At the late gastrula stage, faint signal was detected in the VLCs, in the wall of the archenteron, and in ectoderm cells of the apical plate (Fig. 8). At the pluteus stage, expression was highest in the gut and in PMCs located at the dorsal apex (the future scheidel region). One caveat with respect to our *tgf- $\beta$*  WMISH studies is that because the target mRNA is expressed at low levels, it is difficult to distinguish endogenous expression from background signal. Our data, however, suggest that *tgf- $\beta$*  is expressed by multiple cell types during gastrulation, including PMCs.

We knocked down the expression of TGF- $\beta$  by microinjecting two different non-overlapping, TB-MOs in *S. purpuratus* (the use of

*S. purpuratus*



*L. variegatus*

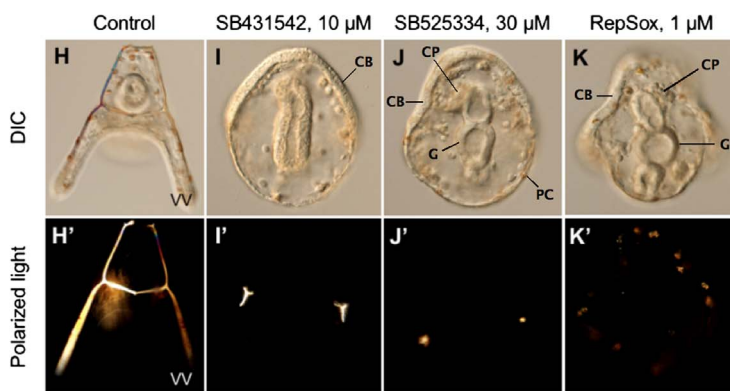


**Fig. 6.** Late Alk4/5/7 activity is required for skeletogenesis in *S. purpuratus* and *L. variegatus*. DIC (A-G) and polarized light (A'-G') images of *S. purpuratus* embryos: a control embryo (A, A') and an embryo exposed to 0.5 μM (B, B') and 5 μM (C, C') SB431542, 1 μM (D, D') and 10 μM (E, E') SB525334, and 0.1 μM (F, F') and 1 μM (G, G') RepSox from the mesenchyme blastula stage (24 hpf) to the prism stage (50 hpf). DIC (H-K) and polarized light (H'-K') images of *L. variegatus* embryos: a control embryo (H, H') and an embryo exposed to 10 μM (I, I') SB431542, 40 μM (J, J') SB525334, and 1 μM (K, K') RepSox from the early gastrula stage to the pluteus stage. The white arrow indicates an anterolateral rod. CB = ciliary band, CP = coelomic pouch, G = tri-partite gut, PC = pigment cell.

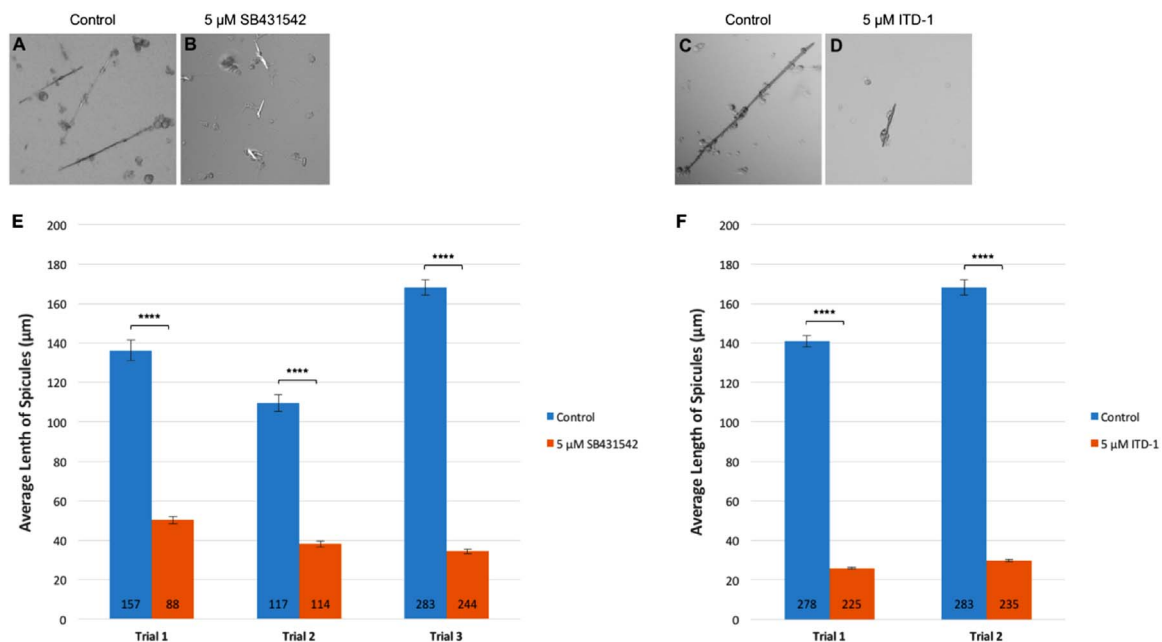


**Fig. 7.** Alk4/5/7 activity and TgfbprtII are required for spicule elongation by PMCs *in vitro*. DIC images of spicules made by the control (A, C), 5 μM SB431542-treated (B) and 5 μM ITD-1-treated (D) micromeres. (E) The average length of spicules made by the control and SB431542-treated micromeres in 3 independent trials is significantly different ( $P < 0.0001$ ). (F) The average length of spicules made by the control and ITD-1-treated micromeres in 2 independent trials is significantly different ( $P < 0.0001$ ). The number at the bottom of each bar indicates the number of spicules quantified. Bars indicate standard errors.

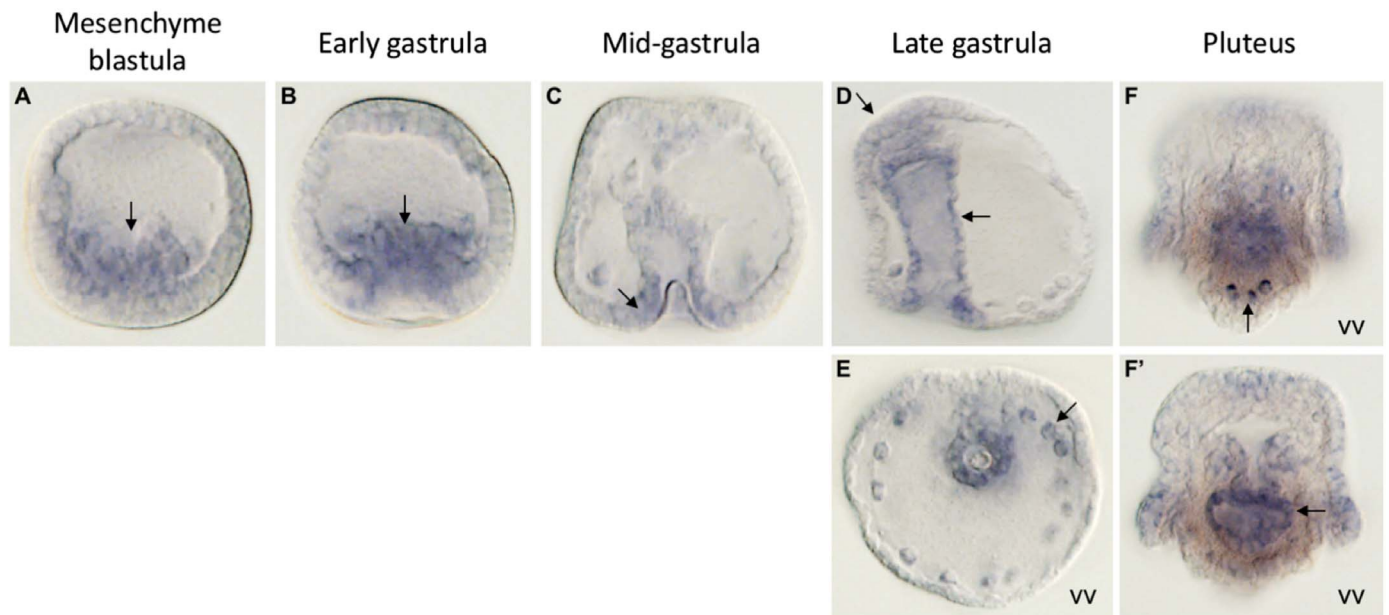


**Fig. 8.** WMISH analysis of *Sp-tgf- $\beta$* . The complete coding sequence of *Sp-tgf- $\beta$*  was used to generate a digoxigenin-labeled probe as described in the Section 2. *tgf- $\beta$*  mRNA is enriched in PMCs at the mesenchyme blastula stage (A, arrow), in the wall of the archenteron at the early and mid-gastrula stages (B, C, arrows), in the VLCs, the wall of the archenteron, and the apical plate ectoderm at the late gastrula stage (D, E, arrows), and in the gut and PMCs in the dorsal apex at the pluteus stage (F, F', arrows). F and F' show two different focal planes of the same embryo. vv = vegetal view.

splice-blocking MOs was problematic in this case due to the exon-intron structure of the *tgf $\beta$ 2* gene). In *S. purpuratus*, more than 80% of embryos injected with 2 mM Sp-TGF- $\beta$  MO-1 (n=107) or 4 mM Sp-TGF- $\beta$  MO-2 (n=103) showed severe inhibition of skeletal elongation (Fig. 9, upper panels). We also knocked down TGF- $\beta$  in *L. variiegatus* using a different TB-MO. Likewise, skeletogenesis was inhibited in *L. variiegatus* embryos injected with 3 mM Lv-TGF- $\beta$  TB-MO (80% of embryos scored, n=93) (Fig. 9, lower panels). In addition to skeletal defects, the gut usually failed to segment in TGF- $\beta$  morphants.

## 4. Discussion

### 4.1. Signaling and skeletal development

The formation of the skeleton is a complex morphogenetic process regulated by multiple signaling pathways. Early (pre-gastrula stage) cues establish territories within the ectoderm and entrain the correct spatial and temporal expression of other signaling ligands that subsequently regulate skeletal morphogenesis. Early axial patterning cues include Nodal, BMP2/4, and other BMP family ligands, which provide information primarily along the dorsal-ventral axis (Molina et al., 2013; Lapraz et al., 2015), and vegetally-derived WNT proteins, which pattern the ectoderm along the anterior-posterior axis (Wei et al., 2012; McIntyre et al., 2013; Range et al., 2013; Cui et al., 2014). These early cues establish within the ectoderm distinct gene regulatory domains and localized signaling centers that regulate skeletal patterning and growth after gastrulation begins. In turn, these localized ectodermal signaling centers create sub-domains of gene expression within the PMC syncytium that likely underlie stereotypical, local variations in skeletal growth rates and morphology (Guss and Ettensohn, 1997; Knapp et al., 2012; Sun and Ettensohn, 2014).

One important consequence of early specification events is the formation of VEGF3 signaling centers at the positions where a subequatorial band of cells known as the border ectoderm intersects the prospective ciliary band. These two sites predict the locations of the future VLCs and skeletal primordia (McIntyre et al., 2014). VEGF3 is a key ectodermal signal that regulates skeletogenesis in multiple ways. This signaling factor acts (directly or indirectly) as an attractant that guides PMC migration, although it is not required for PMC motility *per*

se. In addition, it regulates skeletal growth by mechanisms independent of PMC guidance (Duloquin et al., 2007; Knapp et al., 2012; Adomako-Ankomah and Ettensohn, 2013). During post-gastrula development, VEGF3 is a critically important regulator of skeletogenesis on the ventral side of the embryo; it controls gene expression and biomineral deposition (i.e. the formation of the anterolateral and postoral rods) selectively in the ventral region (Adomako-Ankomah and Ettensohn, 2013; Sun and Ettensohn, 2014). Piacentino et al. (2016b) have shown that sulfated proteoglycans (SPGs) also play a role in the development of ventral skeletal elements (most prominently, the ventral transverse rods) through an effect on PMC positioning, although the possible relationship between SPGs and VEGF3 signaling is not yet clear.

Although VEGF3 plays an essential role, it is not the only signaling molecule that influences skeletogenesis. A requirement for factors other than VEGF3 is highlighted by the finding that recombinant VEGF3 regulates skeletal growth and branching *in vitro* but only when supplemented by fetal bovine serum, which presumably provides other essential factors (Knapp et al., 2012). Another candidate signaling factor is FGF, which shows a dynamic pattern of expression both in the ectoderm and the PMC syncytium (Röttinger et al., 2008; Adomako-Ankomah and Ettensohn, 2013). Knockdowns of FGF in different species have yielded variable results, however. At least in *S. purpuratus* and *L. variiegatus*, this protein appears to play a very limited role in skeletal development (Adomako-Ankomah and Ettensohn, 2013). A different, as yet unidentified, cue is produced locally by ectoderm in the dorsal apex and is responsible for the local up-regulation of many genes in the scheidel-forming domain of the PMC syncytium at late embryonic stages (Sun and Ettensohn, 2014).

### 4.2. TGF- $\beta$ signaling and skeletogenesis

Our studies reveal an essential role for TGF- $\beta$  signaling in skeletogenesis and show that the suite of signaling pathways that regulate skeletogenesis is even more diverse than previously appreciated. The *tgfbrtII* gene is activated selectively in the large micromere-PMC lineage at the late blastula stage as a consequence of inputs from *abx1* and *ets1*, two pivotal regulatory genes in the PMC gene regulatory network (Rafiq et al., 2014). During gastrulation, TgfbrtII acts in

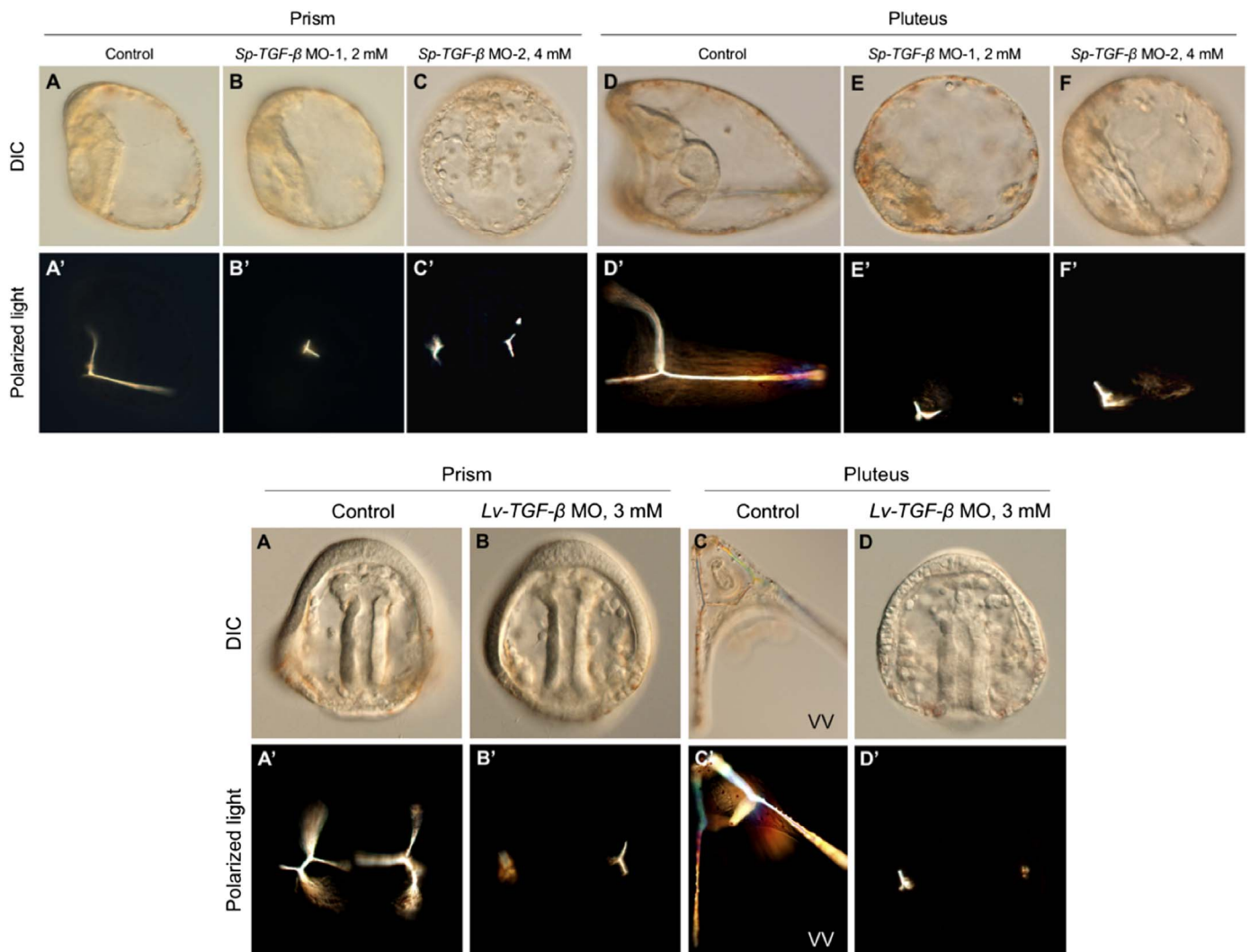


**Fig. 9.** Knockdown of TGF- $\beta$  inhibits skeletal elongation in *S. purpuratus* and *L. variegatus* embryos. Upper panels (*S. purpuratus*): DIC (A-F) and polarized light (A'-F') images of control embryos at the prism stage (A, A') and the pluteus stage (D, D'), embryos injected with 2 mM *Sp-TGF- $\beta$*  translation-blocking MO-1 that had developed to the equivalent of the prism (B, B') and the pluteus stages (E, E'), and embryo injected with 4 mM *Sp-TGF- $\beta$*  translation-blocking MO-2 that had developed to the equivalent of the prism (C, C') or pluteus stage (F, F'). Lower panels (*L. variegatus*): DIC (A-D) and polarized light (A'-D') images of control embryos at the early pluteus stage (A, A') and the late pluteus stage (C, C') and embryos injected with 3 mM *Lv-TGF- $\beta$*  translation-blocking MO that had developed to the equivalent of the prism (B, B') or the late pluteus stage (D, D').

conjunction with its likely cognate type I TGF- $\beta$  receptor, Alk4/5/7, which is more widely expressed (Piacentino et al., 2015), to transduce extrinsic cues required for the deposition of skeletal elements. Thus, one of the consequences of PMC specification, a maternally-entrained, cell autonomous process, is to activate the expression of various membrane receptors (e.g., TgfbtII and Vegfr-Ig10) that mediate the subsequent, cell signal-dependent regulation of gene expression within the PMC syncytium.

Several lines of evidence suggest that TGF- $\beta$  is the ligand that binds TgfbtII. 1) Molecular phylogenetic analysis indicates that TgfbtII is the sea urchin ortholog of human TGF- $\beta$  receptor type II (Lapraz et al., 2006), an assignment supported by specific structural features of the sea urchin protein (this study). In mammals, TGF- $\beta$  receptor type II interacts specifically with TGF- $\beta$  *sensu stricto* (Yadin et al., 2016). 2) The level of *tgf- $\beta$*  mRNA peaks during gastrulation, the critical period for signaling through TgfbtII. 3) Knockdown of TGF- $\beta$  using three different MOs in two sea urchin species shows that this ligand is essential for skeletal growth. We cannot exclude the possibility that, in sea urchins, TGF- $\beta$  also interacts with Acvr2, although such an interaction has not been reported in mammals and our data indicate that if such an interaction occurs it is not sufficient to support skeletogenesis. Although *tgf- $\beta$*  is expressed at relatively low levels,

our WMISH analysis indicates that the gene is expressed in multiple tissues during gastrulation. Unlike VEGF3, *tgf- $\beta$*  is not expressed selectively in discrete subdomains of the ectoderm overlying sites of skeletal growth. Thus, we propose that TGF- $\beta$  provides a non-localized cue that, while absolutely required for skeletal growth, does not impart spatial patterning information to the developing skeleton. According to this view, the formation of a proper skeleton requires an integration of both localized and non-localized cues by the PMC syncytium.

Piacentino et al. (2015) recently reported that SB431542 selectively inhibits the formation of anterior skeletal elements and provided evidence that univin might be the relevant ligand. In our studies, we also observed a selective inhibition of anterior skeletal structures but at concentrations of SB431542 that others have reported are too low to disrupt dorso-ventral polarity or SMAD phosphorylation (Ohguro et al., 2011; Bergeron et al., 2011). We observed that slightly higher concentrations of SB431542, which have been used more routinely to inhibit Alk4/5/7 activity in sea urchins, produced a more complete inhibition of skeletogenesis. We interpret these effects and our other findings as evidence of a much broader role for TGF- $\beta$  signaling in skeletal development and propose that TGF- $\beta$  *sensu stricto* is the relevant ligand. It should be noted, however, that the two interpretations are not mutually exclusive; i.e., it remains possible that, in parallel with the

broader role we find for TGF- $\beta$ -mediated signaling in skeleton formation, univin signaling might contribute selectively to the formation of anterior skeletal structures, as proposed by Piacentino et al. (2015).

The mechanism by which signaling through TgfbtII regulates skeletal growth remains to be elucidated. Signaling through the canonical TGF- $\beta$  pathway is mediated by SMAD2/3 and leads to a transcriptional response. *Sp-smad2/3* mRNA is enriched in PMCs during gastrulation (Poustka et al., 2007; Rafiq et al., 2014), indicating that this transcriptional effector is present at the right time and place to mediate signaling. In vertebrates, TGF- $\beta$  signaling regulates the expression of multiple ECM components that play important roles in the development and maintenance of the skeleton (Ignatz and Massagué, 1986; Noda et al., 1988; Noda, 1989; Wu et al., 2016). Based on these findings, one possible scenario is that TGF- $\beta$  signaling regulates the expression by PMCs of ECM proteins, such as collagens, that are essential for skeletogenesis (Blankenship and Benson, 1984; Butler et al., 1987; Wessel and McClay, 1987; Wessel et al., 1991; Rafiq et al., 2014). TGF- $\beta$  also signals through non-canonical (i.e., SMAD-independent) pathways, however, including the MAPK and PI3K pathways, which can induce rapid cell responses by post-transcriptional mechanisms (Zhang, 2009). The effects of PI3K inhibitors on skeletogenesis *in vivo* and *in vitro* (Bradham et al., 2004) are very similar to the effects of ITD-1 reported here, consistent with a possible link between these two pathways. Our preliminary studies indicate that ITD-1 produces a measurable inhibition of skeletal elongation within 2 h (data not shown), but this does not resolve the question of whether the drug's effect is mediated by transcriptional or post-transcriptional mechanisms. Further studies will be required to determine whether TGF- $\beta$  signaling occurs by canonical or non-canonical pathways (or both), the molecular targets of TGF- $\beta$  signaling, and the specific roles of those proteins in biomineral formation.

## Acknowledgements

This work was supported by National Science Foundation Grant IOS-1354973 to C.A.E.

## Appendix A. Supplementary material

Supplementary data associated with this article can be found in the online version at doi:10.1016/j.ydbio.2016.12.007.

## References

- Adams, D.K., Sewell, M.A., Angerer, R.C., Angerer, L.M., 2011. Rapid adaptation to food availability by a dopamine-mediated morphogenetic response. *Nat. Commun.* 2, 592.
- Adomako-Ankomah, A., Etensohn, C.A., 2011. P58-A and P58-B: novel proteins that mediate skeletogenesis in the sea urchin embryo. *Dev. Biol.* 353, 81–93.
- Adomako-Ankomah, A., Etensohn, C.A., 2013. Growth factor-mediated mesodermal cell guidance and skeletogenesis during sea urchin gastrulation. *Development* 140, 4214–4225.
- Armstrong, N., Hardin, J., McClay, D.R., 1993. Cell-cell interactions regulate skeleton formation in the sea urchin embryo. *Development* 119, 833–840.
- Bergeron, K.F., Xu, X., Brandhorst, B.P., 2011. Oral-aboral patterning and gastrulation of sea urchin embryos depend on sulfated glycosaminoglycans. *Mech. Dev.* 128, 71–89.
- Blankenship, J., Benson, S., 1984. Collagen metabolism and spicule formation in sea urchin micromeres. *Exp. Cell Res.* 152, 98–104.
- Boesen, C.C., Radaev, S., Motyka, S.A., Patamawenu, A., Sun, P.D., 2002. The 1.1 A crystal structure of human TGF-beta type II receptor ligand binding domain. *Structure* 10, 913–919.
- Bradham, C.A., Miranda, E.L., McClay, D.R., 2004. PI3K inhibitors block skeletogenesis but not patterning in sea urchin embryos. *Dev. Dyn.* 229, 713–721.
- Butler, E., Hardin, J., Benson, S., 1987. The role of lysyl oxidase and collagen crosslinking during sea urchin development. *Exp. Cell Res.* 173, 174–182.
- Cheers, M.S., Etensohn, C.A., 2004. Rapid microinjection of fertilized eggs. *Methods Cell Biol.* 74, 287–310.
- Cui, M., Siriwon, N., Li, E., Davidson, E.H., Peter, I.S., 2014. Specific functions of the Wnt signaling system in gene regulatory networks throughout the early sea urchin embryo. *Proc. Natl. Acad. Sci. USA* 111, E5029–E5038.
- Dale, B., Yazaki, I., Tosti, E., 1997. Polarized distribution of L-type calcium channels in early sea urchin embryos. *Am. J. Physiol.* 273, C822–C825.
- Duboc, V., Röttinger, E., Besnardeau, L., Lepage, T., 2004. Nodal and BMP2/4 signaling organizes the oral-aboral axis of the sea urchin embryo. *Dev. Cell* 6, 397–410.
- Duboc, V., Röttinger, E., Lapraz, F., Besnardeau, L., Lepage, T., 2005. Left-right asymmetry in the sea urchin embryo is regulated by nodal signaling on the right side. *Dev. Cell* 9, 147–158.
- Duboc, V., Lapraz, F., Saudemont, A., Bessodes, N., Mekpoh, F., Haillot, E., Lepage, T., 2010. Nodal and BMP2/4 pattern the mesoderm and endoderm during development of the sea urchin embryo. *Development* 137, 223–235.
- Duloquin, L., Lhomond, G., Gache, C., 2007. Localized VEGF signaling from ectoderm to mesenchyme cells controls morphogenesis of the sea urchin embryo skeleton. *Development* 134, 2293–2302.
- Etensohn, C.A., 2013. Encoding anatomy: developmental gene regulatory networks and morphogenesis. *Genesis* 51, 383–409.
- Etensohn, C.A., Dey, D., 2016. Kirrell, a member of the Ig-domain superfamily of adhesion proteins, is essential for fusion of primary mesenchyme cells in the sea urchin embryo. *Dev. Biol.* (Epub ahead of print).
- Etensohn, C.A., McClay, D.R., 1988. Cell lineage conversion in the sea urchin embryo. *Dev. Biol.* 125, 396–409.
- Etensohn, C.A., Malinda, K.M., 1993. Size regulation and morphogenesis: a cellular analysis of skeletogenesis in the sea urchin embryo. *Development* 119, 155–167.
- Flowers, V.L., Courteau, G.R., Poustka, A.J., Weng, W., Venuiti, J.M., 2004. Nodal/activin signaling establishes oral-aboral polarity in the early sea urchin embryo. *Dev. Dyn.* 231, 727–740.
- Galileo, D.S., Morrill, J.B., 1985. Patterns of cells and extracellular material of the sea urchin *Lytechinus variegatus* (Echinodermata: Echinoidea) embryo, from hatched blastula to late gastrula. *J. Morphol.* 185, 387–402.
- Gellibert, F., Woolven, J., Fouchet, M.H., Mathews, N., Goodland, H., Lovegrove, V., Laroze, A., Nguyen, V.L., Sautet, S., Wang, R., Janson, C., Smith, W., Krysa, G., Boullay, V., De Gouville, A.C., Huet, S., Hartley, D., 2004. Identification of 1,5-naphthyridine derivatives as a novel series of potent and selective TGF-beta type I receptor inhibitors. *J. Med. Chem.* 47, 4494–4506.
- Grygielko, E.T., Martin, W.M., Tweed, C., Thornton, P., Harling, J., Brooks, D.P., Laping, N.J., 2005. Inhibition of gene markers of fibrosis with a novel inhibitor of transforming growth factor-beta type I receptor kinase in puromycin-induced nephritis. *J. Pharmacol. Exp. Ther.* 313, 943–951.
- Guss, K.A., Etensohn, C.A., 1997. Skeletal morphogenesis in the sea urchin embryo: regulation of primary mesenchyme gene expression and skeletal rod growth by ectoderm-derived cues. *Development* 124, 1899–1908.
- Gustafson, T., Wolpert, L., 1961. Studies on the cellular basis of morphogenesis in the sea urchin embryo: directed movements of primary mesenchyme cells in normal and vegetalized larvae. *Exp. Cell Res.* 24, 64–79.
- Hardin, J., Coffman, J.A., Black, S.D., McClay, D.R., 1992. Commitment along the dorsoventral axis of the sea urchin embryo is altered in response to NiCl<sub>2</sub>. *Development* 116, 671–685.
- Hart, M.W., Strathmann, R.R., 1994. Functional consequences of phenotypic plasticity in echinoid larvae. *Biol. Bull.* 186, 291–299.
- Hata, A., Chen, Y.G., 2016. TGF- $\beta$  signaling from receptors to Smads. *Cold Spring Harb. Perspect. Biol.* pii: a022061. doi: 10.1101.
- Hodor, P.G., Etensohn, C.A., 2008. Mesenchymal cell fusion in the sea urchin embryo. *Methods Mol. Biol.* 475, 315–334.
- Huminięcki, L., Goldovsky, L., Freilich, S., Moustakas, A., Ouzounis, C., Heldin, C.H., 2009. Emergence, development and diversification of the TGF- $\beta$  signalling pathway within the animal kingdom. *BMC Evol. Biol.* 9, 28.
- Ignatz, R.A., Massagué, J., 1986. Transforming growth factor-beta stimulates the expression of fibronectin and collagen and their incorporation into the extracellular matrix. *J. Biol. Chem.* 261, 4337–4345.
- Inman, G.J., Nicolás, F.J., Callahan, J.F., Harling, J.D., Gaster, L.M., Reith, A.D., Laping, N.J., Hill, C.S., 2002. SB-431542 is a potent and specific inhibitor of transforming growth factor-beta superfamily type I activin receptor-like kinase (ALK) receptors ALK4, ALK5, and ALK7. *Mol. Pharmacol.* 62, 65–74.
- Knapp, R.T., Wu, C.H., Mobilia, K.C., Joester, D., 2012. Recombinant sea urchin vascular endothelial growth factor directs single-crystal growth and branching *in vitro*. *J. Am. Chem. Soc.* 134, 17908–17911.
- Lapraz, F., Röttinger, E., Duboc, V., Range, R., Duloquin, L., Walton, K., Wilson, K., 2006. RTK and TGF- $\beta$  signaling pathways genes in the sea urchin genome. *Dev. Biol.* 300, 132–152.
- Lapraz, F., Haillot, E., Lepage, T., 2015. A deuterostome origin of the Spemann organizer suggested by Nodal and ADMPs functions in Echinoderms. *Nat. Commun.* 6, 8927.
- Luo, Y.J., Su, Y.H., 2012. Opposing nodal and BMP signals regulate left-right asymmetry in the sea urchin larva. *PLoS Biol.* 10, e1001402.
- Massagué, J., 2012. TGF $\beta$  signalling in context. *Nat. Rev. Mol. Cell Biol.* 13, 616–630.
- McClay, D.R., 2016. Sea urchin morphogenesis. *Curr. Top. Dev. Biol.* 117, 15–29.
- McIntyre, D.C., Seay, N.W., Croce, J.C., McClay, D.R., 2013. Short-range Wnt5 signaling initiates specification of sea urchin posterior ectoderm. *Development* 140, 4881–4889.
- McIntyre, D.C., Lyons, D.C., Martik, M., McClay, D.R., 2014. Branching out: origins of the sea urchin larval skeleton in development and evolution. *Genesis* 52, 173–185.
- Molina, M.D., de Crozé, N., Haillot, E., Lepage, T., 2013. Nodal: master and commander of the dorsal-ventral and left-right axes in the sea urchin embryo. *Curr. Opin. Genet. Dev.* 23, 445–453.
- Noda, M., 1989. Transcriptional regulation of osteocalcin production by transforming growth factor- $\beta$  in rat osteoblast-like cells. *Endocrinology* 124, 612–617.
- Noda, M., Yoon, K., Prince, C.W., Butler, W.T., Rodan, G.A., 1988. Transcriptional regulation of osteopontin production in rat osteosarcoma cells by type beta transforming growth factor. *J. Biol. Chem.* 263, 13916–13921.

- Ogunjimi, A.A., Zeqiraj, E., Ceccarelli, D.F., Sicheri, F., Wrana, J.L., David, L., 2012. Structural basis for specificity of TGF $\beta$  family receptor small molecule inhibitors. *Cell Signal* 24, 476–483.
- Ohguro, Y., Takata, H., Kominami, T., 2011. Involvement of Delta and Nodal signals in the specification process of five types of secondary mesenchyme cells in embryo of the sea urchin, *Hemicentrotus pulcherrimus*. *Dev. Growth Differ.* 53, 110–123.
- Pennington, J.T., Strathmann, R.R., 1990. Consequences of the calcite skeletons of planktonic echinoderm larvae for orientation, swimming, and shape. *Biol. Bull.* 179, 121–133.
- Piacentino, M.L., Ramachandran, J., Bradham, C.A., 2015. Late Alk4/5/7 signaling is required for anterior skeletal patterning in sea urchin embryos. *Development* 142, 943–952.
- Piacentino, M.L., Chung, O., Ramachandran, J., Zuch, D.T., Yu, J., Conaway, E.A., Reyna, A.E., Bradham, C.A., 2016a. Zygotic LvBMP5-8 is required for skeletal patterning and for left-right but not dorsal-ventral specification in the sea urchin embryo. *Dev. Biol.* 412, 44–56.
- Piacentino, M.L., Zuch, D.T., Fishman, J., Rose, S., Speranza, E.E., Li, C., Yu, J., Chung, O., Ramachandran, J., Ferrell, P., Patel, V., Reyna, A., Hameeduddin, H., Chaves, J., Hewitt, F.B., Bardot, E., Lee, D., Core, A.B., Hogan, J.D., Keenan, J.L., Luo, L., Coulombe-Huntington, J., Blute, T.A., Oleinik, E., Ibn-Salem, J., Poustka, A.J., Bradham, C.A., 2016b. RNA-seq identifies SPGs as a ventral skeletal patterning cue in sea urchins. *Development* 143, 703–714.
- Poustka, A.J., Kühn, A., Groth, D., Weise, V., Yaguchi, S., Burke, R.D., Herwig, R., Lehrach, H., Panopoulou, G., 2007. A global view of gene expression in lithium and zinc treated sea urchin embryos: new components of gene regulatory networks. *Genome Biol.* 8, R85.
- Rafiq, K., Shashikant, T., McManus, C.J., Ettensohn, C.A., 2014. Genome-wide analysis of the skeletogenic gene regulatory network of sea urchins. *Development* 141, 950–961.
- Range, R., Lapraz, F., Quirin, M., Marro, S., Besnardeau, L., Lepage, T., 2007. Cis-regulatory analysis of nodal and maternal control of dorsal-ventral axis formation by Univin, a TGF- $\beta$  related to Vg1. *Development* 134, 3649–3664.
- Range, R.C., Angerer, R.C., Angerer, L.M., 2013. Integration of canonical and noncanonical Wnt signaling pathways patterns the neuroectoderm along the anterior-posterior axis of sea urchin embryos. *PLoS Biol.* 11, e1001467.
- Röttinger, E., Saudemont, A., Duboc, V., Besnardeau, L., McClay, D., Lepage, T., 2008. FGF signals guide migration of mesenchymal cells, control skeletal morphogenesis and regulate gastrulation during sea urchin development. *Development* 135, 353–365.
- Sethi, A.J., Angerer, R.C., Angerer, L.M., 2009. Gene regulatory network interactions in sea urchin endomesoderm induction. *PLoS Biol.* 7, e1000029.
- Sharma, T., Ettensohn, C.A., 2011. Regulative deployment of the skeletogenic gene regulatory network during sea urchin development. *Development* 138, 2581–2590.
- Strathmann, R.R., 1971. The feeding behavior of planktotrophic echinoderm larvae: mechanisms, regulation, and rates of suspension-feeding. *J. Exp. Mar. Biol. Ecol.* 6, 109–160.
- Strathmann, R.R., Grünbaum, D., 2006. Good eaters, poor swimmers: compromises in larval form. *Int. Comp. Biol.* 46, 312–322.
- Sun, Z., Ettensohn, C.A., 2014. Signal-dependent regulation of the sea urchin skeletogenic gene regulatory network. *Gene Expr. Patterns* 16, 93–103.
- Tu, Q., Cameron, R.A., Worley, K.C., Gibbs, R.A., Davidson, E.H., 2012. Gene structure in the sea urchin *Strongylocentrotus purpuratus* based on transcriptome analysis. *Genomes Res.* 22, 2079–2087.
- Tu, Q., Cameron, R.A., Davidson, E.H., 2014. Quantitative developmental transcriptomes of the sea urchin *Strongylocentrotus purpuratus*. *Dev. Biol.* 385, 160–167.
- Wei, Z., Range, R., Angerer, R., Angerer, L., 2012. Axial patterning interactions in the sea urchin embryo: suppression of nodal by Wnt1 signaling. *Development* 139, 1662–1669.
- Wessel, G.M., McClay, D.R., 1987. Gastrulation in the sea urchin embryo requires the deposition of crosslinked collagen within the extracellular matrix. *Dev. Biol.* 121, 149–165.
- Wessel, G.M., Etkin, M., Benson, S., 1991. Primary mesenchyme cells of the sea urchin embryo require an autonomously produced, nonfibrillar collagen for spiculogenesis. *Dev. Biol.* 148, 261–272.
- Willems, E., Cabral-Teixeira, J., Schade, D., Cai, W., Reeves, P., Bushway, P.J., Lanier, M., Walsh, C., Kirchhausen, T., Izpisua Belmonte, J.C., Cashman, J., Mercola, M., 2012. Small molecule-mediated TGF- $\beta$  type II receptor degradation promotes cardiomyogenesis in embryonic stem cells. *Cell Stem Cell* 11, pp. 242–252.
- Wilt, F.H., Benson, S.C., 2004. Isolation and culture of micromeres and primary mesenchyme cells. *Methods Cell Biol.* 74, 273–285.
- Wilt, F.H., Ettensohn, C.A., 2007. Morphogenesis and biomineralization of the sea urchin larval endoskeleton. In: Bauerlein, E. (Ed.), *Handbook of Biomineralization*. Wiley-VCH Press, Weinheim, Germany, 183–210.
- Wu, M., Chen, G., Li, Y.-P., 2016. TGF- $\beta$  and BMP signaling in osteoblast, skeletal development, and bone formation, homeostasis and disease. *Bone Res.* 4, 16009.
- Wu, M.Y., Hill, C.S., 2009. Tgf-beta superfamily signaling in embryonic development and homeostasis. *Dev. Cell* 16, 329–343.
- Yadin, D., Knaus, P., Mueller, T.D., 2016. Structural insights into BMP receptors: specificity, activation and inhibition. *Cytokine Growth Factor Rev.* 27, 13–34.
- Yaguchi, S., Yaguchi, J., Burke, R.D., 2006. Specification of ectoderm restricts the size of the animal plate and patterns neurogenesis in sea urchin embryos. *Development* 133, 2337–2346.
- Zhang, Y.E., 2009. Non-Smad pathways in TGF-beta signaling. *Cell Res.* 19, 128–139.
- Zito, F., Costa, C., Sciarino, S., Poma, V., Russo, R., Angerer, L.M., Matranga, V., 2003. Expression of univin, a TGF-beta growth factor, requires ectoderm-ECM interaction and promotes skeletal growth in the sea urchin embryo. *Dev. Biol.* 264, 217–227.